ACS Catalysis

Letter

pubs.acs.org/acscatalysis

Efficient Electrocatalytic Water Oxidation by a Copper Oxide Thin Film in Borate Buffer

Fengshou Yu,[†] Fei Li,*[,†] Biaobiao Zhang,[†] Hua Li,[†] and Licheng Sun*[,†,‡]

[†]State Key Laboratory of Fine Chemicals, DUT-KTH Joint Education and Research Center on Molecular Devices, Dalian Universityof Technology (DUT), 116024 Dalian, China

[‡]Department of Chemistry, School of Chemical Science and Engineering, KTH Royal Institute of Technology, 10044 Stockholm,Sweden

Supporting Information

ABSTRACT: A robust water oxidation catalyst based on copper oxide was prepared by facile electrodeposition of Cu^{2+} from borate buffer solution under near neutral conditions. The Cu−B_i thin film exhibits high activity and long-term stability in Cu^{2+}-free pH 9 borate buffer. A steady current density of 1.2 mA/cm^2 was sustained for at least 10 h at 1.3 V versus NHE without iR compensation, which sets a new benchmark for copper-based OEC.

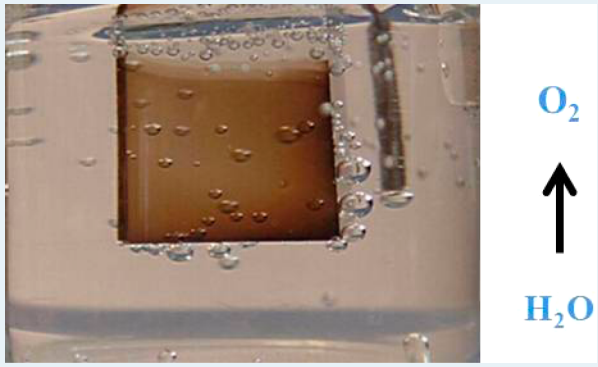

KEYWORDS: *water splitting, copper, electrocatalysis, water oxidation, thin film*

Solar energy conversion and storage have attracted worldwide attention due to its importance to the rising global energy demand and environmental concerns. A renewable and sustainable method to address these questions is to split water into oxygen and hydrogen powered by sunlight directly or indirectly.[1] In general, water splitting is hindered by the oxidation of water to oxygen due to its demanded 4e$^-$, 4H$^+$ processes. To overcome this obstacle, the robust, low-cost water oxidation catalysts that perform fast oxygen evolution at low overpotentials and benign conditions are highly desired.[2] In this regard, electrodeposited amorphous cobalt and nickel oxides possess attractive properties in preparation, activity, and longevity for electrocatalytic water oxidation under near-neutral conditions.[3−7] Besides these earth-abundant elements, copper is an attractive low cost metal, which has been used for solar energy conversion. For example, Cu_2O is a well-known p-type semiconductor with a narrow band gap of 2.0 eV and relatively high absorption coefficient in the visible region.[8] Nanostructured Cu_2O and CuO have been prepared as efficient photocathodes for hydrogen evolution.[9−14] Cu_2O as a photocatalyst for overall water splitting has also been reported.[15] However, Cu_2O is prone to undergo oxidative or reductive photocorrosion to form CuO or Cu, which inhibit its wide application in photocatalysis. On the other hand, copper-based electrocatalysts have not been much concerned in the area of water splitting. It is only recently that a handful of molecular copper complexes have been shown to electrocatalyze water oxidation in aqueous solutions.[16−19] A major drawback for these homogeneous systems is that highly alkaline media (>pH 10) are imperative to oxygen generation due to the high overpotentials required by copper complexes (>750 mV).

Although a nanostructured CuO electrodeposited from molecular copper(II) 2-pyridylmethylamine complex was reported by Du to be an active catalyst toward electrochemical water oxidation,[20] we report here the first example of copper-based oxygen-evolving catalyst (OEC) easily prepared by electrodepostion from the Cu^{2+} salt solution in borate electrolyte at pH 9 (B_i). The in situ formed copper oxide thin film is inert to corrosion and exhibits high catalytic activity with the steady current densities up to 1.2 mA/cm^2 at 1.3 V versus NHE without iR compensation in borate buffer.

Cyclic voltammogram (CV) scans of a GC working electrode with and without Cu^{2+} in borate electrolyte at pH 9 are shown in Figure 1a. For the first scan, a prominent catalytic wave above background due to water oxidation was observed with the onset potential ($E_{p,o}$) at 1.2 V (all potentials are reported versus the normal hydrogen electrode).[21] A weak broad reduction wave centered at $E_{p,a}$ = 1.0 V was observed in the subsequent reverse scan, which is caused by the reduction of a surface species generated by the anodic sweep.[6,18] The continued CV scans show stepped increased catalytic and anodic wave currents, and the onset cathodically shifts to 1.1 V.

Received: October 2, 2014
Revised: December 4, 2014
Published: December 17, 2014

DOI: 10.1021/cs501510e
ACS Catal. 2015, 5, 627−630

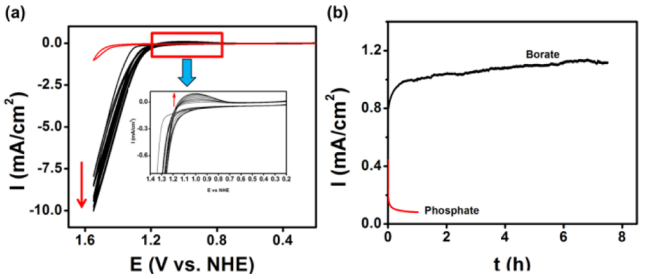

Figure 1. (a) Successive CV scans obtained from a solution of 1 mM $Cu(NO_3)_2$ in 0.2 M borate buffer with glassy carbon as a working electrode (0.07 cm^2), Ag/AgCl as a reference electrode, and Pt as a counter electrode, with a scan rate of 100 mV/s. The CV trace in the absence of Cu^{2+} is shown in red. The inset shows magnified views of the continually increasing reduction waves. (b) Current density trace of electrodeposition of Cu−B_i film on FTO substrate at a constant potential of 1.3 V (versus NHE) in 0.2 M borate buffer containing 1 mM Cu^{2+} at pH 9 (black line). The red line shows the current density trace in a pH 9 phosphate buffer.

These observations are consistent with the formation of surface deposited materials, indicative of the growth of a solid active film. After 10 scans, the peak current of 10 mA/cm^2 was obtained at 1.5 V with a scan rate of 100 mV/s. Similar CV behavior was observed by the solid thin film using an FTO substrate.

In order to fabricate an anode, electrolysis was carried out in borate buffer in the presence of 1 mM Cu^{2+} with a constant bias of 1.3 V, which results in a stably rising current density associated with the formation of a dark brown coating film on FTO-coated glass slide bearing an active area of 1 cm^2. The current density reaches a steady value of 1 mA cm^{-2} after electrolysis for 7 h with a passed charge of 25 C/cm^2, indicating an equilibrium between the solution species and the surface species. The formation of Cu-OEC closely resemble those of the reported Co-OEC and Ni-OEC,[3,6] the choice of the suitable proton-accepting electrolyte is essential to form stable film and to maintain a high activity.[22,23] Control experiments showed no film formation in the absence of borate electrolyte or replacing the borate buffer with phosphate buffer (Figure 1b). It should be noted that slow addition of $Cu(NO_3)_2$ into borate to avoid the precipitation of $Cu(BO_2)_2$ from solution is necessary to prepare the electrolyte for electrodeposition.

Scanning-electron microscopy (SEM) images of the deposit reveal an compact amorphous layer covered with spheroidal nodules, the particles size are in the range of 100−300 nm (Figure 2a). SEM image also indicates an average thickness of 200 nm for the film prepared at 1.3 V for 7 h (Figure 2b). The composition of the thin film was analyzed by energy dispersive

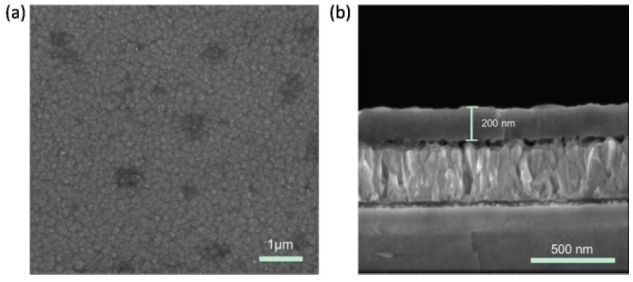

Figure 2. SEM images of the eletrodeposited Cu−B_i film from the top view (a) and the profile view (b).

X-ray analysis (EDX) (Figure S1), indicating a Cu/B/O ratio of 2:1:12. X-ray photoelectron spectroscopy (XPS) spectrum exhibits two satellite peaks at 942.3 and 961.8 eV (Figure S2), indicative of the oxidation state of Cu(II) for the surface species. The determined binding energy of 954.0 and 933.9 eV are assigned to Cu $2p_{1/2}$ and Cu $2p_{3/2}$, which are higher than those for Cu(0) metal and consistent with CuO.[24] In our case, $Cu(OH)_2$ was ruled out, which has been reported to exhibit $2p_{1/2}$ and $2p_{3/2}$ peaks at 955.2 and 935.1 eV, respectively.[25] Since B appears to be a minor component in the thin film, the structure of copper borate electrocatalyst (Cu−B_i) was proposed to be dominated by CuO.

In view of practical application, the activity of the Cu−B_i film with a thickness of 200 nm was further examined in a Cu^{2+}-free borate buffer (pH 9). Constant potential electrolysis at 1.3 V leads to a steady current density sustained at 1.2 mA/cm^2 (Figure 3). This value is comparable to that performed in the

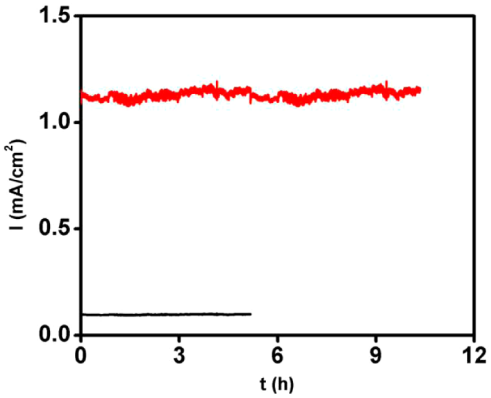

Figure 3. Current density traces obtained by controlled-potential electrolysis of the FTO electrodes (1 cm^2) coated and without (black line) and with Cu−B_i catalytic film (red line) in stirred 0.2 M Cu^{2+}-free borate buffer solution (pH 9) at 1.3 V vs NHE.

presence of $Cu(NO_3)_2$ (Figure 1b) and thus excludes the contribution of dissolved Cu^{2+} to the observed activity. In a continued electrolysis for 10 h, neither current density decrease nor electrode corrosion was found. Furthermore, the electrode showed identical CVs before and after bulk electrolysis, confirming that Cu−B_i is indeed a robust OEC (Figure S3). EDX and XPS were performed after 10 h of electrolysis, which exhibited essentially identical spectra to the initial ones (Figure S1 and S2). As shown in Figure S4, the activity of Cu−B_i was compared with those of Co−B_i and Ni−B_i films prepared by the literature methods.[3,6] Under our test conditions at 1.3 V, the activity of Cu−B_i is comparable to that of Ni−B_i (1.4 mA/cm^2) but lower than that of Co−B_i (2.1 mA/cm^2).

The electrochemical behavior of Cu−B_i is different with the copper oxide film precipitated from Na_2CO_3 solution of Cu^{2+}, as has been recently noted by Meyer and co-workers.[18] The reported film was found to be unstable in Cu^{2+}-free Na_2CO_3 solution. Bulk electrolysis at 1.3 V resulted in rapid dissolution of the precipitation and the current density dropped significantly to 30% of the initial level within 1 h (Figure S5). These observations again highlight the crucial role of buffering electrolyte on maintaining the equilibrium between dissolution and precipitation of metal ion under anodic potentials. In another experiment, the amount of evolved O_2 over the period of electrolysis was collected and measured to be 63 μM, which

DOI: 10.1021/cs501510e
ACS Catal. 2015, 5, 627−630

accounts for a Faradaic efficiency of 95% in comparison with the passed charge of 25.5 C (Figure S6).

The steady-state current density (j) was evaluated as a function of overpotential in stirred borate buffers (Figure 4a).

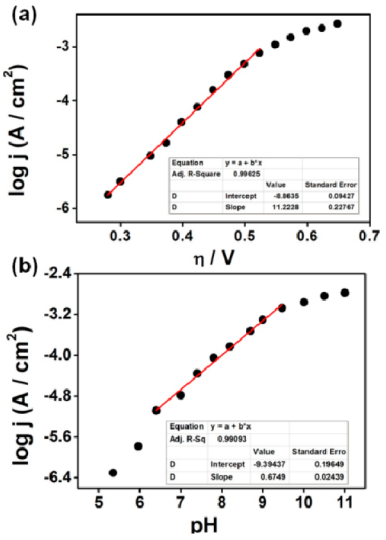

Figure 4. (a) Tafel plot of Cu−B_i film in 0.2 M borate buffer at pH 9 with iR compensation. (b) Current density dependence on pH value at 1.2 V vs NHE in 0.2 M borate buffer without iR compensation.

By plotting overpotential as a function of log j, a Tafel slope of 89 mV/decade was obtained, which is larger than 59 mV/decade for Co−P_i and Ni−B_i.[3,26a] Since the thick film may raise the internal barriers of electron and mass transport and results in higher Tafel slopes, a thinner film was prepared by electrodeposition with a passage of 1 C/cm^2. Anodization has been previously demonstrated to improve the catalytic activity of Ni−B_i through the subtle changes of the oxidation state and the structure of metal oxide cluster.[26b] Upon bulk electrolysis of the 1 C/cm^2 Cu−B_i, we noticed a similar effect on this film: When anodizing the film at 1.3 V in pH 9 borate buffer, the current density increased for 3 h until reaching a plateau (Figure S7). However, the Tafel plot of the thinner film exhibited a similar slope to that of 200 nm, 25 C/cm^2 film, indicating the intrinsic properties of Cu−B_i OEC are not significantly altered by film thickness.

The dependence of current density on pH value was explored in the range of pH 5−11 (Figure 4b). A linear relationship between log j and pH values was displayed between pH 6.5−9.5, giving a slope of 0.67 decade/pH. Past this pH, the slope derivates from linearity probably due to the mechanism change by switching the reactant from water to hydroxyl ion.[27] Within the pH range of 6.5−9.5, the pH dependence of overpotential was deduced to be −60 mV/pH based on eq 1,[28] which is close to the value of −58.4 mV/pH obtained from galvanostatic experiment (Figure S8). This value also agrees with the Nernstian behavior, suggesting ne$^-$/nH$^+$ transfer prior to a chemical rate-determing step.

$$\left(\frac{\partial E}{\partial \mathrm{pH}}\right)_j = -\left(\frac{\partial \log j}{\partial \mathrm{pH}}\right)_E \left(\frac{\partial E}{\partial \log j}\right)_{\mathrm{pH}} \quad (1)$$

In summary, a stable copper oxide thin film was demonstrated to be a highly active electrocatalyst for water oxidation in near-neutral conditions. This heterogeneous OEC was fabricated by electrodeposition of Cu^{2+} in borate buffer solution at pH 9, reminiscent of the in situ formed Co−P_i and Ni−B_i from proton buffering solutions. The high activity at relatively low overpotential, the easy accessibility, and benign working conditions of Cu−B_i provide obvious advantages over the reported copper-based OEC.

■ ASSOCIATED CONTENT

Supporting Information

The following file is available free of charge on the ACS Publications website at DOI: 10.1021/cs501510e.

Experimental section, EDX and XPS spectra (PDF)

■ AUTHOR INFORMATION

Corresponding Authors

*E-mail: lifei@dlut.edu.cn.

*E-mail: lichengs@kth.se.

Notes

The authors declare no competing financial interest.

■ ACKNOWLEDGMENTS

This work was supported by the National Basic Research Program of China (2014CB239402), the National Natural Science Foundation of China (21476043, 21120102036, 21361130020), the Natural Science Foundation of Liaoning Province, China (2014020010), the Fundamental Research Funds for the Central Universities (DUT14YQ104), the Swedish Energy Agency and the K&A Wallenberg Foundation.

■ REFERENCES

(1) Youngblood, W. J.; Lee, S. A.; Maeda, K.; Mallouk, T. E. *Acc. Chem. Res.* **2009**, *42*, 1966−1973.

(2) Walter, M. G.; Warren, E. L.; McKone, J. R.; Boettcher, S. W.; Mi, Q.; Santori, E. A.; Lewis, N. S. *Chem. Rev.* **2010**, *110*, 6446−6473.

(3) Kanan, M. W.; Nocera, D. G. *Science* **2008**, *321*, 1072−1075.

(4) Joya, K. S.; Takanabe, K.; de Groot, H. J. M. *Adv. Energy Mater.* **2014**, *4*, article no. 1400252 10.1002/aenm.201470086

(5) Han, A.; Wu, H.; Sun, Z.; Jia, H.; Du, P. *Phys. Chem. Chem. Phys.* **2013**, *15*, 12534−1538.

(6) Dinca, M.; Surendranath, Y.; Nocera, D. G. *Proc. Natl. Acad. Sci. U.S.A.* **2010**, *107*, 10337−10341.

(7) Wang, D.; Ghirlanda, G.; Allen, J. P. *J. Am. Chem. Soc.* **2014**, *136*, 10198−10201.

(8) (a) Akimoto, K.; Ishizuka, S.; Yanagita, M.; Nawa, Y.; Paul, G. K.; Sakurai, T. *Sol. Energy* **2006**, *80*, 715−722. (b) Izaki, M.; Shinagawa, T.; Mizuno, K.; Ida, Y.; Inaba, M.; Tasaka, A. *J. Phys. D: Appl. Phys.* **2007**, *40*, 3326−3329.

(9) Bandara, J.; Udawatta, C. P. K.; Rajapakse, C. S. K. *Photochem. Photobiol. Sci.* **2005**, *4*, 857−861.

(10) Choi, H.; Kang, M. *Int. J. Hydrogen Energy* **2007**, *32*, 3841−3848.

(11) Paracchino, A.; Laporte, V.; Sivula, K.; Grätzel, M.; Thimsen, E. *Nat. Mater.* **2011**, *10*, 456−461.

(12) Zhai, Q.; Xie, S.; Fan, W.; Zhang, Q.; Wang, Y.; Deng, W.; Wang, Y. *Angew. Chem., Int. Ed.* **2013**, *52*, 5776−5779.

(13) Bornoz, P.; Abdi, F. F.; Tilley, S. D.; Dam, B.; van de Krol, R.; Graetzel, M.; Sivula, K. *J. Phys. Chem. C* **2014**, *118*, 16959−16966.

(14) Qian, F.; Wang, G.; Li, Y. *Nano Lett.* **2010**, *10*, 4686−4691.

(15) Hara, M.; Kondo, T.; Komoda, M.; Ikeda, S.; Kondo, J. N.; Domen, K. *Chem. Commun.* **1998**, 357−358.

(16) Barnett, S. M.; Goldberg, K. I.; Mayer, J. M. *Nat. Chem.* **2012**, *4*, 498−502.

(17) Zhang, T.; Wang, C.; Liu, S.; Wang, J. L.; Lin, W. *J. Am. Chem. Soc.* **2014**, *136*, 273−281.

(18) Chen, Z.; Meyer, T. J. *Angew. Chem., Int. Ed.* **2013**, *52*, 700−703.

DOI: 10.1021/cs501510e
ACS Catal. 2015, 5, 627−630

(19) Zhang, M.; Chen, Z.; Kang, P.; Meyer, T. J. *J. Am. Chem. Soc.* **2013**, *135*, 2048−2051.
(20) Liu, X.; Jia, H.; Sun, Z.; Chen, H.; Xu, P.; Du, P. *Electrochem. Commun.* **2014**, *46*, 1−6.
(21) The onset potential was determined from the intersection of two tangents drawn at the rising and background current of the cyclic voltammogram. Alhalash, W.; Holze, R. *J. Solid State Electrochem* **2007**, *11*, 1605−1612.
(22) Surendranath, Y.; Dincă, M.; Nocera, D. G. *J. Am. Chem. Soc.* **2009**, *131*, 2615−2620.
(23) Gerken, J. B.; Landis, E. C.; Hamers, R. J.; Stahl, S. S. *ChemSusChem.* **2010**, *3*, 1176−1179.
(24) Durando, M.; Morrish, R.; Muscat, A. J. *J. Am. Chem. Soc.* **2008**, *130*, 16659−16668.
(25) McIntyre, N. S.; Sunder, S.; Shoesmith, D. W.; Stanchell, F. W. *J. Vac. Sci. Technol.* **1981**, *18*, 714.
(26) (a) Bediako, D. K.; Surendranath, Y.; Nocera, D. G. *J. Am. Chem. Soc.* **2013**, *135*, 3662−3674. (b) Bediako, D. K.; Lassalle-Kaiser, B.; Surendranath, Y.; Yano, J.; Yachandra, V. K.; Nocera, D. G. *J. Am. Chem. Soc.* **2012**, *134*, 6801−6809.
(27) Michael, A.; Ioannis, K.; Josef, C. M.; Sebastian, O. K.; P. Ulrich, B.; Angel, A. T.; Michael, R.; Karl, J. J. M. *Phys. Chem. Chem. Phys.* **2011**, *15*, 16384−16394.
(28) Surendranath, Y.; Lutterman, D. A.; Liu, Y.; Nocera, D. G. *J. Am. Chem. Soc.* **2012**, *134*, 6326−6336.

DOI: 10.1021/cs501510e
ACS Catal. 2015, 5, 627−630